PROTEINS
STRUCTURE ■ FUNCTION ■ BIOINFORMATICS

SHORT COMMUNICATION

Pentacoordinated phosphorus revisited by high-level QM/MM calculations

Enrique Marcos,[1] Martin J. Field,[2] and Ramon Crehuet[1]*

[1]Departament de Química Biològica i Modelització Molecular, Institut de Química Avançada de Catalunya (CSIC), Barcelona, Spain

[2]Laboratoire de Dynamique Moléculaire, Institut de Biologie Structurale, CNRS-CEA-UJF, Grenoble, France

ABSTRACT

Enzymes catalyzing phosphoryl transfer reactions are extremely efficient and are involved in crucial biochemical processes. The mechanisms of these enzymes are complex due to the diversity of substrates that are involved. The reaction can proceed through a pentacoordinated phosphorus species that is either a stable intermediate or a transition state (TS). Because of this, the first X-ray structure of a pentacoordinated phosphorus intermediate in the β-phosphoglucomutase enzyme aroused great interest but also much controversy. To provide new insights into the nature of that structure, we have determined the reaction path of the phosphorylation step using high-level QM/MM calculations, and have also calculated the geometry of a complex with a transition state analogue (TSA) that has been suggested to be the actual species in the crystal. The protein crystalline environment has been modeled so as to mimic the experimental conditions. We conclude that the pentacoordinated phosphorus formed in this enzyme is not a stable species but a TS, which gives an activation energy for phosphorylation in agreement with kinetic results. We also show that the TSA is a good mimic of the true TS. We have performed a new crystallographic refinement of the original diffraction map of the pentacoordinated phosphorus structure with the MgF_3^- TSA. The new fit improves significantly with respect to the original one, which strongly supports that Allen and coworkers wrongly assigned the X-ray structure to a pentavalent phosphorane.

Proteins 2010; 78:2405–2411.

Key words: enzyme catalysis; NEB; pentacoordinated phosphorus; phosphorylation; QM/MM; phosphoglucomutase.

INTRODUCTION

The phosphoryl transfer reaction is ubiquitous in nature.[1] However, its mechanism is still the subject of debate because nucleophilic substitution in phosphorus is more complex than in carbon or other first row elements.[2] Understanding the mechanism of this reaction and the elucidation of possible intermediates is crucial for the design of enzyme inhibitors, which often provide the starting points for the development of new drugs.[3]

In 2003, the first X-ray structure of a pentacoordinated phosphorus intermediate was published.[4] It corresponded to a phosphoryl transfer between a glutamate residue and β-glucose-6-phosphate (G6P) in the β-phosphoglucomutase enzyme (β-PGM) to give β-glucose-1,6-bisphosphate (β-G16BP). This structure was highly controversial and it stimulated several comments[5,6] and both computational[7,8] and experimental[9–12] studies. In particular, the existence of a phosphoryl moiety in the crystal was questioned. It was suggested that the position of the PO_3^{2-} fragment was actually occupied by an MgF_3^- ion formed under crystallization conditions.[5] This was supported by Webster's calculations,[7] which showed that the pentacoordinated species was the transition state (TS) separating the tetracoordinated reactant and product phosphates. These results were subsequently challenged by Allen and coworkers,[9] who claimed that a phosphoryl was present in the active site based on quantitative analytical methods. Subsequent NMR[10,11] and kinetic[12] experiments

Additional Supporting Information may be found in the online version of this article.

Grant sponsor: Spanish MEC; Grant number: CTQ2009-08223; Grant sponsor: Catalan AGAUR; Grant number: 2005SGR00111; Grant sponsor: JAE Program of the Consejo Superior de Investigaciones Científicas (CSIC)

*Correspondence to: Ramon Crehuet, Departament de Química Biològica i Modelització Molecular, Institut de Química Avançada de Catalunya (CSIC), c/Jordi Girona 18-26, E-08034 Barcelona, Spain. E-mail: ramon.crehuet@iqac.csic.es

Received 16 December 2009; Revised 15 April 2010; Accepted 19 April 2010
Published online 28 April 2010 in Wiley InterScience (www.interscience.wiley.com).
DOI: 10.1002/prot.22758

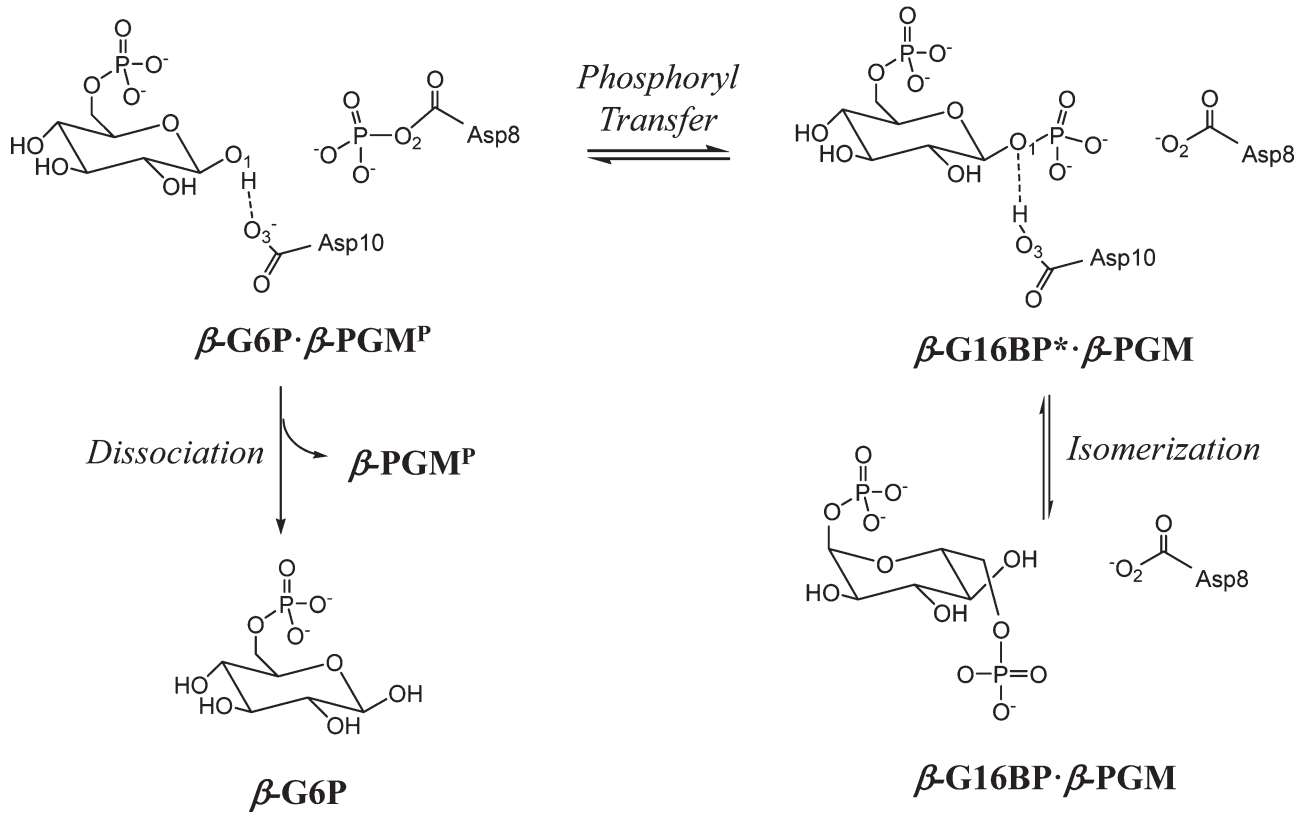

Figure 1

Reaction scheme for the reaction of β-PGM complexed with β-G16BP.

in solution carried out by Waltho and coworkers eventually confirmed that the MgF_3^- ion is a transition state analogue (TSA) that replaces the phosphoryl moiety. These studies raised the question of how well the TSA mimics the geometry and interactions of the true TS.[12] The kinetic study[12] determined the overall rate for the process shown in Figure 1 in which β-G16BP, which can be in two conformations in equilibrium, phosphorylates the enzyme to render a β-G6P·β-PGM^P complex that subsequently undergoes a fast dissociation. The measured rate constant involved the phosphorylation step and product complex dissociation, but whether it also involved isomerization between the equilibrium conformations of the β-G16BP·β-PGM complex could not be ascertained from the kinetic experiments. Likewise the identity of the rate limiting step could not be determined. The activation energy calculated by Webster[7] was much higher than that indicated by the measured kinetic data for the set of steps that included phosphoryl transfer. Was this discrepancy due to the accuracy of the theoretical models employed or is the crystal structure different from the conformation in solution within which the phosphoryl transfer takes place?

In this communication, we revisit the mechanism of the phosphoryl transfer catalyzed by the enzyme β-PGM and compare it with the geometry of the MgF_3^- complex. We report the results of hybrid QM/MM reaction path calculations and put special emphasis on the accuracy of the techniques employed. This is also a feature of the work of other authors. Several studies[13–23] have stated the importance of using very precise quantum chemical methods to describe the kinetic and thermodynamic stability of potential pentacoordinated intermediates. Moreover, Warshel and coworkers[18–23] have also highlighted the need to analyze the free energy surface to describe the reaction paths of phosphoryl transfers. In addition, we have also tried to ensure that the electrostatic effect of the crystal environment on the active site region is properly represented.

MATERIALS AND METHODS

The coordinates of the enzyme were obtained from the crystallographic structure with PDB id.1O08. Hydrogen atoms were added to the structure with standard protonation states at pH = 7, and Asp8 and Asp10 were protonated according to Fig. 1. Geometry optimizations were then performed on the structure. In these, the positions of the atoms were constrained with harmonic forces

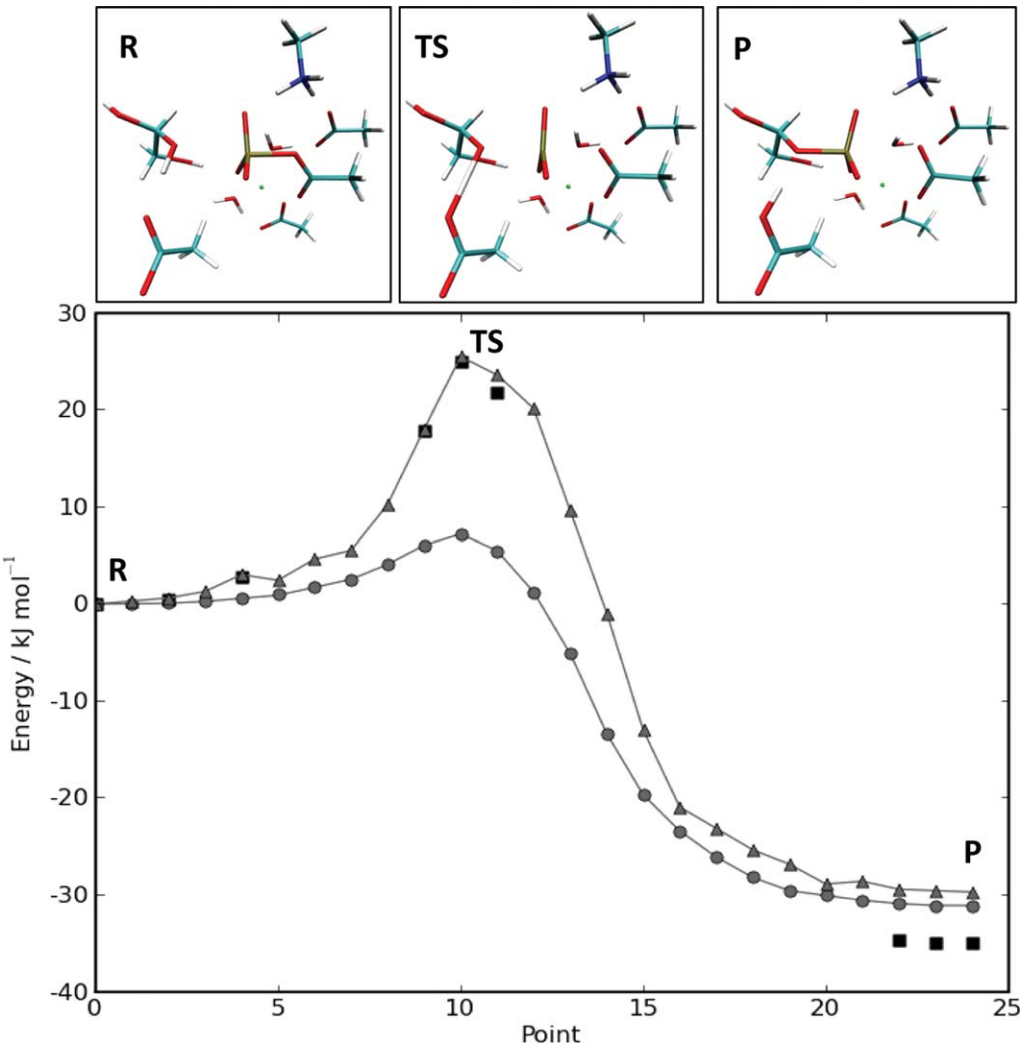

Figure 2

The most reliable energy profile in this work was obtained at the levels of theory *m*PW1PW/b2/q2 (triangles), and SCS-MP2/b2/q2 (squares) with the NEB method. For the latter, only the structures around the stationary points were calculated. More calculations that illustrate convergence to this final profile can be found in the supporting information. The *x*-axis corresponds to structures along the reaction path separated by a constant length. The structures of the QM region of the reactant, transition state, and product are also displayed (the atomic coordinates are given in the Supporting Information).

that were progressively relaxed. We did not perform molecular dynamics simulations as we wanted the structure to remain as close as possible to the experimental one.

For the QM/MM calculations, the system was partitioned between QM and MM regions as depicted in Figure 4. A small QM region was used for the geometry optimizations and nudged elastic band (NEB) calculations. This is denoted q1 in the text and had 58 atoms. A larger QM region, q2, with 94 atoms was employed for single point calculations to verify the results with q1.

A comparison and assessment of the different methods can be found in the Supporting Information. The best estimates are obtained with methods **m7** and **m8**, and these are the ones that are discussed hereafter.

The OPLS-AA force field[24] was employed for the MM region whereas the SCS-MP2[25] and different DFT methods were used for the QM region. Geometry optimizations and NEB calculations were performed with the *m*PWPW functional,[26] which has been parameterized to describe noncovalent interactions. Our previous calculations[16] have shown the good performance of the hybrid version of this functional (*m*PW1PW)[26] in describing the geometry and energetics of pentacoordinated phosphorus compounds. The results of this work (see Supporting Information) show that the pure and hybrid DFT functionals give similar geometries but that the calculations for the former are much faster because of the use of the resolution of the identity approximation. The

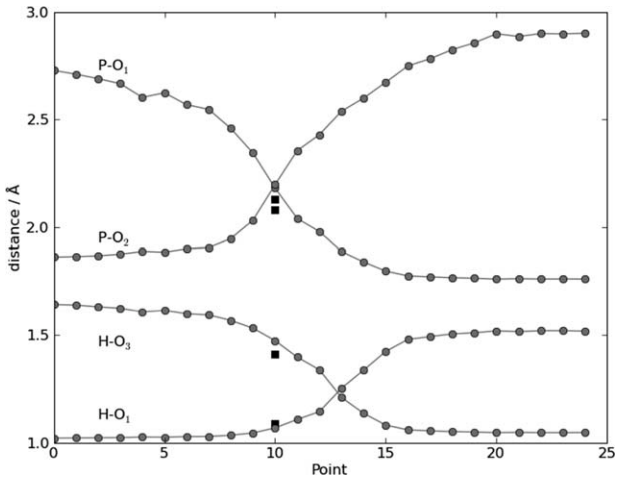

Figure 3

Variations of some relevant distances along the reaction path (gray circles). We also depict the analogous distances in the MgF_3^- TSA complex (black squares). The atomic coordinates of the TSA complex are given in the Supporting Information.

basis set used for the optimization was Ahlrichs-VDZ[27] with polarization functions on nonhydrogen atoms, and a diffuse function on oxygen.[28] It is denoted b1 in the text. Single point calculations were performed with b1 and also a larger Ahlrichs-VTZ[27,29] basis with polarization and diffuse functions on all atoms.[28,30] This is denoted b2. All the system setup and the QM/MM calculations were performed with the pDynamo software[31] using a modified version of the interface to the ORCA program,[32–34] which was employed for the QM calculations.

The reaction path was optimized with the NEB method[35–38] implemented in pDynamo. The utility of NEB can be seen from inspection of Figure 3 in which four distances change asynchronously along the reaction path. Such behavior is obtained automatically in a NEB calculation, but is difficult or impossible to reproduce using a predefined set of reaction coordinate variables.

The MgF_3^- TSA complex was constructed by substitution of the PO_3^- moiety in both reactant and product structures. Subsequent optimizations revealed a convergence to a unique structure as discussed below. In the crystallographic refinement, the four new atoms were treated independently as unbound atoms. A new structure was obtained after several cycles of anisotropic B_{factor} restrained refinement using the program REFMAC[39] yielding a final improved R_{factor} of 12.8%, and an R_{free} of 16.9%. The final 2Fo-Fc electron density map fitting can be seen in Supporting Information Figure S3.

For the crystal calculations, the periodic images of the molecule were generated with Pymol[40] (see Supporting Information Fig. S1). OPLS-AA MM charges on the atoms were used to represent the electrostatic field of the first-shell protein molecules, whereas for more distant periodic copies of the protein a dipolar representation was employed. Full details are given in the Supporting Information.

RESULTS AND DISCUSSION

Our results indicate that the pentacoordinated phosphorus is not a stable species. The complete energy profile that we calculate for the reaction is given in Figure 2, and the reactant and product species are depicted in Figure 1. Although we looked for additional intermediates, including those with different protonation states, that could lead to an alternative stepwise mechanism,[21] the only two stable species that are predicted to occur are those depicted in Figure 1 (phosphorylation step). In relation to this, Waltho and coworkers showed that the β-PGM enzyme prioritizes anionic charge over geometry in aluminum and magnesium fluoride TS analogs.[11] Therefore, the deprotonated form of the phosphoryl moiety, which bears a −1 formal charge, will be preferred over other protonation states. In support of this, we have been unable to locate a stable pentacoordinated intermediate, either with the deprotonated form or with forms in which different oxygen of the phosphoryl moiety are protonated.

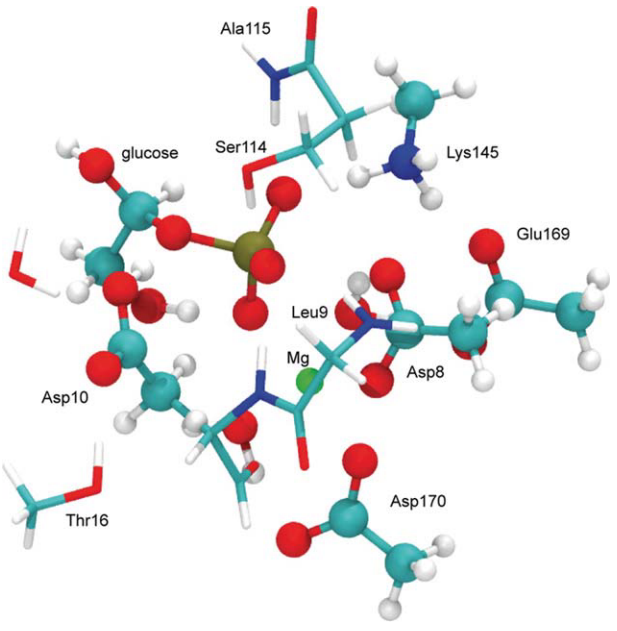

Figure 4

QM regions used in this work: q1 (ball and stick) and the larger q2 (sticks only). The MM region is constituted by all the remaining atoms in the crystal structure, including the water molecules. No additional water molecules were added. Environmental effects due to the crystal were simulated by the addition of periodic protein images as described in the main text and Supporting Information. This figure was created with VMD.[41]

In the reactants, the P atom is bound to the O2 carboxylic oxygen of the aspartate residue (Asp8) at a distance of 1.86 Å, whereas the glucose O1 atom is at 2.73 Å from P. This cannot be considered a pentacoordinated structure as it differs significantly from the crystal structure, in which the P—O1 and P—O2 distances are 2.0 and 2.1 Å, respectively. Likewise, the P atom is not pentacoordinated in the products, as it is bound to glucose O1 at a distance of 1.76 Å (the latter having been deprotonated by Asp10) and is at 2.90 Å from the Asp8 oxygen. The shorter P—O distance in the products is because hydroxylate is a better nucleophile than carboxylate.[16] This, together with the nature of the proton-accepting group, accounts for the exothermicity of 35.0–29.7 kJ mol^{-1} that we observe for the reaction.

Figure 2 shows that the reaction has a single TS with an energy barrier of 24.9–25.5 kJ mol^{-1} with respect to reactants. The TS corresponds to a pentacoordinated species with P—O1 and P—O2 distances of 2.18 and 2.19 Å, respectively (see Fig. 3). Clearly, this species cannot correspond to the one that is observed in the crystal structure as it is unstable.

Figure 3 illustrates the variation in certain interatomic distances along the reaction path and shows that nucleophilic attack occurs before proton transfer. This is better understood by considering the reaction in the reverse direction. The carboxylate group of Asp8 is a weak nucleophile, all the more so when it is coordinated with Mg^{2+}. As such it can only attack the phosphate when the glucose oxygen is protonated, because this hydroxyl is then also a weak nucleophile of similar strength. Figure 3 also shows the interatomic distances for the TSA complex in which an Mg atom replaces P. It is worth emphasizing that the MgF_3 complex and the structure of the TS have strikingly similar bond distances between the central atom and the nucleophile and leaving groups. Remarkably, the distances for the G6P proton that is transferred to Asp10 are also in close agreement with that of the TS. The main difference lies in the Mg—F bond distances, which we predict to be in the range of 1.91–1.94 Å, whereas the equivalent P—O distances in the calculated TS structure are 1.53–1.56 Å. (see Supporting Information Fig. S2 for a comparison between both structures). The reported P—O distances in the PDB are 1.66–1.70 Å. This disagreement led us to analyze the original experimental diffraction map of structure 1O08. We refined the structure using an MgF_3 moiety in place of the PO_3 without constraining its bond distances. The fit is improved using MgF_3 with respect to the original PO_3 (see "Materials and Methods" section and Supporting Information Figure S3). The optimized distances are now in the range of 1.85–1.91 Å, in close agreement with the calculated ones. Therefore, the density map fitting also supports our computational result that MgF_3^- is the species present in the active site.

In the kinetic study by Waltho and coworkers a rate constant was obtained (k = 105 s^{-1}) for the formation of β-G6P from the β-G16BP·β-PGM complex (see Fig. 1), but they were unable to assign this rate constant to a specific step. A direct application of TS theory gives an upper value for the activation free energy for the process of 61.5 kJ mol^{-1}. It is worth reminding the reader that the calculated energy profile shown in Figure 2 corresponds to the phosphoryl transfer step of the inverted process, that is, the formation of β-G16BP·β-PGM from β-G6P·β-PGM^P. Therefore, if we make the approximation of equating free energy with potential energy, we can compare the energy difference between the TS and products with the experimental energy barrier (61.5 kJ mol^{-1}). This value is in very good agreement with our findings, which gives a result of 55.2–59.9 kJ mol^{-1} using our best two calculation methods, **m7** and **m8**. Thus, we can identify the experimental rate constant as arising from the chemical process of phosphoryl transfer, and conclude that the remaining processes will be faster (or as fast as) this step. Webster's results gave an energy barrier for this process of 76.6 kJ mol^{-1}, which is in less good agreement with the experimental rate constant. It is not obvious to ascertain the reasons for the discrepancy between Webster's result and ours, given the differences in computational procedures between the two studies (e.g., the functional, basis sets, number of degrees of freedom that are minimized, the embedding between the high and low-level parts of the model, etc.). Although a difference of 15 kJ mol^{-1} cannot be considered large, the better agreement of our value with the experimental one and its relative insensitivity to parameter changes (see Supporting Information), provide support for the validity of our computational approach.

Waltho and coworkers also studied the kinetics of inhibition with fluoride and magnesium. They concluded that the ions first enter an open form of the enzyme, which then closes tightly.[12] This open-close motion of the enzyme is important for turnover and product release (see Fig. 1). The good agreement for the phosphoryl transfer activation energy is proof that MgF_3^- is a good TSA, that is, that the structure in the crystal is close to the conformation that forms β-G16BP in solution. The matching geometries of the calculated PO_3^- and MgF_3^- complexes also suggest that the latter can be a better TSA than other commonly used ones, such as vanadate, which sometimes fails to reproduce the same interactions as the actual TS in other kinases.[12] Further agreement with experiment can be obtained with the calculated NMR chemical shifts for the fluorine in the active site: −213, −203, and −195 ppm. Although the absolute values differ, the relative values compare well with the measured ones[10]: −159, −152, and −147 ppm. Again, this confirms that the crystal structure contains MgF_3^- in a conformation close to that in solution. Details of these calculations are reported in the Supporting Information.

We have already stated the importance of having a converged calculation, both in terms of the quality of the

Table I
Relative Energies of Reactants, TS and Products in kJ mol^{-1}

Name	Method[a]	Reactants	TS[b]	Products
m7	*m*PW1PW/b2/q2	0.0	25.5	−29.7
m8	SCS-MP2/b2/q2	0.0	24.9	−35.0
m9	SCS-MP2/b2/q2[c]	0.0	27.8	−21.3
m10	SCS-MP2/b2/q2[d]	0.0	27.2	−24.1

[a]The QM method, the basis set, and the QM region used is shown.
[b]The energy of structure 10 of the reaction path.
[c]Including the point charges of the 14 neighboring molecules.
[d]Same as footnote "c" plus the dipoles of 6897 neighboring molecules.

method used for the quantum mechanical region and in its size. Figure 4 shows the two QM regions that were used, one for the optimization, and the larger one for the best energy profile. Our best results are listed in Table I. Supporting Information discusses the validity of this choice with additional results.

The results discussed so far correspond to calculations with an isolated enzyme molecule. In the crystal, periodic effects can create a different electrostatic environment. Because of the importance of polarizability effects in pentacoordinated phosphorus species, the electrostatic field generated by the crystal could potentially change the energetics of the profile.[16–18] To investigate this point, we included, as a first step, the point charges of the first shell of 14 protein molecules that surround the one under study (**m9**). And, in a second step, we added the dipole moments of the 6897 closest crystal images of the central protein beyond the first shell (**m10**, see Supporting Information for details). Table I shows that these environments do not change significantly the results for a single molecule. We also hypothesize that solvent effects will have a minor influence, because the active site of this molecule is buried far from the solvent.

CONCLUSIONS

In the present investigation, we have analyzed the structure reported by Allen and coworkers[4] in their crystallographic study of the β-phosphoglucomutase enzyme, both with respect to the reaction mechanism of phosphoryl transfer and the geometry of the MgF_3^- TSA complex. To have a proper theoretical description of the reacting species during phosphoryl transfer, we have employed a series of high-level QM/MM simulation models, and we have also used a number of representations of the protein's crystalline environment so as to reproduce the experimental conditions as closely as possible. Our results reveal that the rate limiting step for the production of G6P from the phosphorylated enzyme is the chemical process of phosphoryl transfer, with an activation energy that corresponds well to the experimental rate constant obtained by Waltho and coworkers. Although we conclude that having a stable, pentacoordinated phosphorus intermediate for this enzyme is impossible, we have shown that the MgF_3^- present in the crystal structure is a good TSA that can give insight into the geometry of the phosphoryl transfer TSs. The good agreement between the experimental and calculated energy barrier and chemical shifts supports our conclusion that the crystal structure is equivalent to the closed conformation that binds the β-G16BP in solution.

ACKNOWLEDGMENTS

This work has been supported by grants from the JAE-predoc programme of the Consejo Superior de Investigaciones Científicas (CSIC), the Spanish MEC (CTQ2009-08223) and the Catalan AGAUR (2005SGR00111). The calculations were performed, in part, with CESCA and CESGA resources. The authors thank Xavier Carpena for help and suggestions in the analysis of the crystallographic data and one of the referees whose comments helped to improve the article.

REFERENCES

1. Cleland WW, Hengge AC. Enzymatic mechanisms of phosphate and sulfate transfer. Chem Rev 2006;106:3252–3278.
2. Allen KN, Dunaway-Mariano D. Phosphoryl group transfer: evolution of a catalytic scaffold. Trends Biochem Sci 2004;29:495–503.
3. Cohen P. The role of protein phosphorylation in human health and disease—delivered on June 30th 2001 at the FEBS Meeting in Lisbon. Eur J Biochem 2001;268:5001–5010.
4. Lahiri SD, Zhang GF, Dunaway-Mariano D, Allen KN. The pentacovalent phosphorus intermediate of a phosphoryl transfer reaction. Science 2003;299:2067–2071.
5. Blackburn GM, Williams NH, Gamblin SJ, Smerdon SJ. Comment on "The pentacovalent phosphorus intermediate of a phosphoryl transfer reaction." Science 2003;301:1184.
6. Allen KN, Dunaway-Mariano D. Response to comment on "The pentacovalent phosphorus intermediate of a phosphoryl transfer reaction." Science 2003;301:1184.
7. Webster CE. High-energy intermediate or stable transition state analogue: theoretical perspective of the active site and mechanism of beta-phosphoglucomutase. J Am Chem Soc 2004;126:6840–6841.
8. Berente I, Beke T, Naray-Szabo G. Quantum mechanical studies on the existence of a trigonal bipyramidal phosphorane intermediate in enzymatic phosphate ester hydrolysis. Theor Chem Acc 2007; 118:129–134.
9. Tremblay LW, Zhang GF, Dai JY, Dunaway-Mariano D, Allen KN. Chemical confirmation of a pentavalent phosphorane in complex with beta-phosphoglucomutase. J Am Chem Soc 2005;127:5298–5299.
10. Baxter NJ, Olguin LF, Golicnik M, Feng G, Hounslow AM, Bermel W, Blackburn GM, Hollfelder F, Waltho JP, Williams NH. A Trojan horse transition state analogue generated by MgF3-formation in an enzyme active site. Proc Natl Acad Sci USA 2006;103:14732–14737.
11. Baxter NJ, Blackburn GM, Marston JP, Hounslow AM, Cliff MJ, Bermel W, Williams NH, Hollfelder F, Wemmer DE, Waltho JP. Anionic charge is prioritized over geometry in aluminum and magnesium fluoride transition state analogs of phosphoryl transfer enzymes. J Am Chem Soc 2008;130:3952–3958.
12. Golicnik M, Olguin LF, Feng GQ, Baxter NJ, Waltho JP, Williams NH, Hollfelder F. Kinetic analysis of beta-phosphoglucomutase and its inhibition by magnesium fluoride. J Am Chem Soc 2009;131: 1575–1588.

13. Elsasser B, Valiev M, Weare JH. A dianionic phosphorane intermediate and transition states in an associative A(N)+D-N mechanism for the ribonuclease A hydrolysis reaction. J Am Chem Soc 2009;131:3869–3871.
14. de Vivo M, Dal Peraro M, Klein ML. Phosphodiester cleavage in ribonuclease H occurs via an associative two-metal-aided catalytic mechanism. J Am Chem Soc 2008;130:10955–10962.
15. Range K, McGrath MJ, Lopez X, York DM. The structure and stability of biological metaphosphate, phosphate, and phosphorane compounds in the gas phase and in solution. J Am Chem Soc 2004;126:1654–1665.
16. Marcos E, Crehuet R, Anglada JM. Inductive and external electric field effects in pentacoordinated phosphorus compounds. J Chem Theory Comput 2008;4:49–63.
17. Marcos E, Anglada JM, Crehuet R. Description of pentacoordinated phosphorus under an external electric field: which basis sets and semi-empirical methods are needed? Phys Chem Chem Phys 2008;10:2442–2450.
18. Klahn M, Rosta E, Warshel A. On the mechanism of hydrolysis of phosphate monoesters dianions in solutions and proteins. J Am Chem Soc 2006;128:15310–15323.
19. Rosta E, Kamerlin SCL, Warshel A. On the interpretation of the observed linear free energy relationship in phosphate hydrolysis: a thorough computational study of phosphate diester hydrolysis in solution. Biochemistry 2008;47:3725–3735.
20. Kamerlin SCL, Florian J, Warshel A. Associative versus dissociative mechanisms of phosphate monoester hydrolysis: on the interpretation of activation entropies. Chem Phys Chem 2008;9:1767–1773.
21. Kamerlin SCL, Williams NH, Warshel A. Dineopentyl phosphate hydrolysis: evidence for stepwise water attack. J Org Chem 2008;73:6960–6969.
22. Kamerlin SCL, Haranczyk M, Warshel A. Are mixed explicit/implicit solvation models reliable for studying phosphate hydrolysis? A comparative study of continuum explicit and mixed solvation models. Chem Phys Chem 2009;10:1125–1134.
23. Kamerlin SCL, McKenna CE, Goondman MF, Warshel A. A computational study of the hydrolysis of dGTP analogues with halomethylene-modified leaving groups in solution: implications for the mechanism of DNA polymerases. Biochemistry 2009;48:5963–5971.
24. Jorgensen WL, Maxwell DS, Tirado-Rives J. Development and testing of the OPLS all-atom force field on conformational energetics and properties of organic liquids. J Am Chem Soc 1996;118:11225–11236.
25. Grimme S. Improved second-order Moller-Plesset perturbation theory by separate scaling of parallel- and antiparallel-spin pair correlation energies. J Chem Phys 2003;118:9095–9102.
26. Adamo C, Barone V. Exchange functionals with improved long-range behavior and adiabatic connection methods without adjustable parameters: the mPW and mPW1PW models. J Chem Phys 1998;108:664–675.
27. Schafer A, Horn H, Ahlrichs R. Fully optimized constracted gaussian-basis sets for atoms Li to Kr. J Chem Phys 1992;97:2571–2577.
28. Krishnan R, Binkley JS, Seeger R, Pople JA. Self-consistent molecular-orbital methods. 20. Basis set fro correlated wave-functions. J Chem Phys 1980;72:650–654.
29. Weigend F, Ahlrichs R. Balanced basis sets of split valence, triple zeta valence and quadruple zeta valence quality for H to Rn: design and assessment of accuracy. Phys Chem Chem Phys 2005;7:3297–3305.
30. McLean AD, Chandler GS. Contracted gaussian-basis sets for molecular calculations. I. 2nd row atoms. $Z = 11$–18. J Chem Phys 1980;72:5639–5648.
31. Field MJ. The pDynamo program for molecular simulations using hybrid quantum chemical and molecular mechanical potentials. J Chem Theory Comput 2008;4:1151–1161.
32. Neese F. ORCA—an ab initio, Density Functional and Semiempirical program package, version 2.6. Bonn: University of Bonn; 2008.
33. Neese F, Wennmohs F, Hansen A, Becker U. Efficient, approximate and parallel Hartree-Fock and hybrid DFT calculations. A 'chain-of-spheres' algorithm for the Hartree-Fock exchange. Chem Phys 2009;356:98–109.
34. Neese F. An improvement of the resolution of the identity approximation for the formation of the Coulomb matrix. J Comput Chem 2003;24:1740–1747.
35. Jónsson H, Mills G, Jacobsen KW. Nudged elastic band method for finding minimum energy paths of transitions. In: Berne BJ, Ciccotti G, Coker DF, editors. Classical and Quantum Dynamics in Condensed Phase Simulations. Singapore: World Scientific; 1998. pp 385–404.
36. Henkelman G, Jónsson H. Improved tangent estimate in the nudged elastic band method for finding minimum energy paths and saddle points. J Chem Phys 2000;113:9978–9985.
37. Crehuet R, Field MJ. A temperature-dependent nudged-elastic-band algorithm. J Chem Phys 2003;118:9563–9571.
38. Galvan IF, Field MJ. Improving the efficiency of the NEB reaction path finding algorithm. J Comput Chem 2008;29:139–143.
39. Murshudov GN, Vagin AA, Dodson EJ. Refinement of macromolecular structures by the maximum-likelihood method. Acta Crystallogr Sect D-Biol Crystallogr 1997;53:240–255.
40. DeLano WL. The PyMOL molecular graphics system. San Carlos, CA: DeLano Scientific; 2002.
41. Humphrey W, Dalke A, Schulten K. VMD: visual molecular dynamics. J Mol Graph 1996;14:33–38.